HVAC&R Research
Publication details, including instructions for authors and subscription information:
http://www.tandfonline.com/loi/uhvc20

A Novel Condensate-Free Refrigerated Cold Plate for Electronic Cooling

Yu-Lieh Wu , Kai-Shing Yang [a] , Min-Yi Chen [b] & Chi-Chuan Wang [c d]

[a] Department of Refrigeration, Air Conditioning and Energy Engineering , National Chin-Yi University of Technology , Taiping City, Taiwan

[b] Department of Electro-Optical and Energy Engineering , MingDao University , Changhua, Taiwan

[c] Environment Research Laboratories , Industrial Technology Research Institute , Hsinchu, Taiwan

[d] Department of Mechanical Engineering , National Chiao Tung University , Hsinchu, Taiwan

Published online: 22 Feb 2011.

To cite this article: Yu-Lieh Wu , Kai-Shing Yang , Min-Yi Chen & Chi-Chuan Wang (2010) A Novel Condensate-Free Refrigerated Cold Plate for Electronic Cooling, HVAC&R Research, 16:1, 3-14

To link to this article: http://dx.doi.org/10.1080/10789669.2010.10390889

A Novel Condensate-Free Refrigerated Cold Plate for Electronic Cooling

Yu-Lieh Wu, PhD **Kai-Shing Yang, PhD**
Min-Yi Chen **Chi-Chuan Wang, PhD**
Fellow ASHRAE

Received April 27, 2009; accepted October 9, 2009

A novel cooling design featuring a two-stage expansion process is proposed in this study. Without any help from insulation, the design can minimize or even entirely eliminate condensate formation outside the cold-plate surface even for a very low evaporation temperature. The design incorporates a double-pipe inlet/outlet and a two-container cold plate, and its performance is compared to a conventional cold plate. For the conventional cold plate, the outlet pressure/temperature hold quite steadily at a light heat load, and the outlet pressure/temperature shows a substantial rise when the refrigerant is completely evaporated. The outlet pressure/temperature of the condensate-free cold plate shows an opposite trend at a heavy heat loading. The benefit of this characteristic is that the wall surface temperature and the outlet temperature of the cold plate can be maintained comparatively more steady than the conventional cold plate.

INTRODUCTION

Currently complementary metal-oxide semiconductor (CMOS) chip technologies act as the major class of integrated circuits and are widely applied in microprocessors, microcontrollers, static random-access memory (RAM), and other digital logic circuits. With the ongoing rise of capability, there is a strong demand for cooling to ensure the performance of microprocessors, microcontrollers, static RAM, and other digital logic circuits. In particular, it is known that the performance of CMOS can be drastically improved if the temperature can be further reduced. There are many advantages (Ghibaudo et al. 1992), e.g., higher carrier mobility, higher saturation velocity, better turn-on capabilities (sub-threshold slope), latch-up immunity, improved reliability due to activated degradation processes, reduced power consumption, a decrease in leakage currents, a lowering of interconnection resistance, increased thermal conductivity, and a reduction of thermal noise, in addition to the low temperature operation.

Moreover, it is well known that operating semiconductor devices at lower temperatures leads to conspicuously improved performance (Taut et al. 1997). This is because of faster switching times of semiconductor devices and increased circuit speeds due to lower electrical resistance of interconnecting materials at low-temperature operations (Balestra and Ghibaudo 1994). Depending on the doping characteristics, attainable performance improvements range from 1% to 3% for every 10°C (50°F) lower transistor temperature (Phelan 2001). However, in addition to the physical limit of shrinking the size of the integrated circuit, the accompanied heat generation becomes

Yu-Lieh Wu is an assistant professor and **Min-Yi Chen** is a graduate student of the Department of Refrigeration, Air Conditioning and Energy Engineering, National Chin-Yi University of Technology, Taiping City, Taiwan. **Kai-Shing Yang** is an assistant professor of the Department of Electro-Optical and Energy Engineering, MingDao University, Changhua, Taiwan. **Chi-Chuan Wang** is a senior lead researcher of Energy & Environment Research Laboratories, Industrial Technology Research Institute, Hsinchu, Taiwan, and a professor in the Department of Mechanical Engineering, National Chiao Tung University, Hsinchu, Taiwan.

more and more difficult to manage. In fact, advanced electronic products all suffer from the rapid rise of cooling demand. Although conventional air cooling still dominates the cooling solutions, it suffers problems such as noise and lower heat transfer performance; hence, alternatives such as heat pipes, liquid immersion, jet impingement and sprays, thermoelectrics, and refrigeration (Trutassanawin et al. 2006) must be considered. Of the available alternatives, only thermoelectrics and refrigeration can provide a sub-ambient operation that is quite attractive for high-flux applications. In practice, refrigeration is capable of operating at a high-temperature ambient, yet its coefficient of performance (COP) is well above the present thermoelectrics system. There are also other advantages for exploiting refrigeration cooling (Taut et al. 1997), such as maintenance of low junction temperatures while dissipating high heat fluxes, potential increases in microprocessor performance at lower operating temperatures, and increased chip reliability. Investigations reported for cooling of electronic devices via refrigeration were mainly related to the fundamental system performance, such as junction to ambient air thermal resistance, system COP of the refrigeration system (Phelan and Swanson 2004), and transient response behavior (Nnann 2006). Some refrigeration cooling systems for electronics are already available (e.g., see Schmidt and Notohardjono [2002], Thermaltake [2009], and Bash et al. [2002]).

However, as pointed out by Agwu Nnanna (2006), there are two major concerns when using refrigeration systems to cool electronics. The first is associated with the condensation on the surfaces subject to sub-ambient operation, and the second is the system's lagging response to applied load at the evaporator. Note that condensation takes place when the temperature is below the dew-point temperature of the surrounding air. The presence of water condensate can bring hazards to the electronic system and must be avoided at all times. Typical solutions may involve clumsy insulation or use an additional heater to vaporize condensate outside the cold plate (Asetek 2009). The former requires considerable space that is often quite limited in practice and is apt to reduce the overall system performance due to blockage of the airflow. The latter design not only raises problems in control but also incurs additional energy consumption. In view of the shortcomings of these two common solutions, the present study offers a novel design to entirely eradicate the influence of condensate. Performance of the proposed concept is then compared with the conventional cold plate.

NOVEL CONCEPT TO MINIMIZE/ELIMINATE CONDENSATE

A refrigeration system normally has four major components, namely a compressor, a condenser, an expansion device, and an evaporator (a cold plate placed above the heat source for heat removal). For this study, the refrigeration system includes a variable-speed drive compressor, a water-cooled condenser, a metering valve and a capillary tube as the expansion device, and a cold plate as the evaporator. R-134a is used as the working refrigerant.

The most crucial design of this concept lies in the process of the pressure-reducing device. During the pressure-reducing process, refrigerant temperature is also reducing. For the conventional design, a low temperature well below the ambient temperature is achieved through an expansion device (capillary tube, expansion valve, short tube, and the like), resulting in a surface temperature lower than the corresponding dew-point temperature. Therefore, condensation takes place on the surface if there is no thermal insulation. To tackle this problem, we have proposed a two-stage expansion design that is capable of minimizing or even entirely eliminating the formation of condensate along the cold plate without the help of insulation. The basic principle of this novel idea can be seen from the T-S diagram shown in Figure 1. The idea incorporates the two-stage expansion in the cold plate. For the first stage of expansion, a capillary tube (or expansion valve) with a shorter length is placed after the condenser, thereby giving rise to a moderate pressure drop of the refrigerant from the condenser. For the second stage of expansion, a two-container cold plate as shown in Figure 2a is fabricated. As seen, the temperature of the

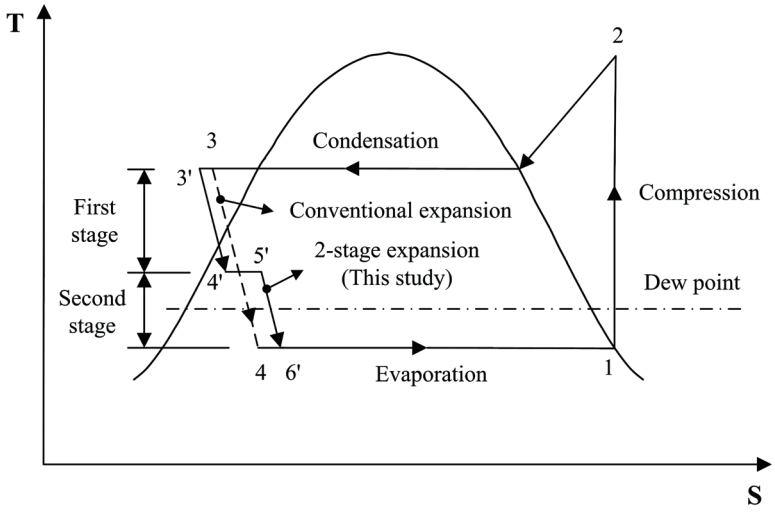

Figure 1. T-S diagram of the present two-stage expansion vs. conventional expansion.

refrigerant from the first-stage expansion caused by the capillary tube is designated to be above the corresponding dew-point temperature of the ambient environment. As a consequence, no condensate forms outside the surface of the cold plate since the temperature is above the dew point. Inside the first container of the cold plate, as seen in Figure 2a, the refrigerant then passes through a short tube to perform the second-stage expansion. The short tube is embedded in the wall of the second container. As the refrigerant flows through the short tube, its temperature is further reduced to be below the dew-point temperature, leading to a much larger temperature difference within the second container while the temperature of the refrigerant at the first container is still above the dew-point temperature. Inside the second container, pin fin array is used to augment the heat transfer. Notice that with this design, the refrigerant flowing through the first or the second container can effective carry heat from the heat source. For complete removal of condensate formation from the whole refrigeration system, the present design places a double-pipe inlet/outlet at the cold plate, with the warmer refrigerant flowing into the cold plate at the outer tube while the colder refrigerant vapor leaving the cold plate is placed in the inner tube. Through this design, the entire refrigeration system, including piping, is free from condensation formation.

EXPERIMENTAL SETUP

A schematic of the whole experimental system is shown in Figure 3. The system is basically a refrigeration system, including a variable-speed drive compressor, a double-pipe condenser, a metering valve and a capillary tube as the expansion device, a cold plate as the evaporator, and an after evaporator to avoid any liquid compression. The mini-rotary compressor has an outer cylinder diameter of 60 mm (2.36 in.) and a length of 100 mm (3.94 in.). The total weight of the compressor is 1.2 kg (2.65 lb_m). The mini compressor is an R-134a-based direct current (DC) driven compressor with an adjustable cooling capacity ranging from 50 to 250 W (0.0474 to 0.23696 Btu/s) and the condenser is a water-cooled double-pipe condenser.

During the operation, water is circulated at the annulus of the double-pipe condenser while refrigerant is flowing inside the tube. A manually controlled metering expansion valve is located at the exit of the condenser. For more easily manipulating and stabilizing the system performance, an extra capillary tube with an inner diameter (ID) of 1 mm (0.0394 in.) and a length of

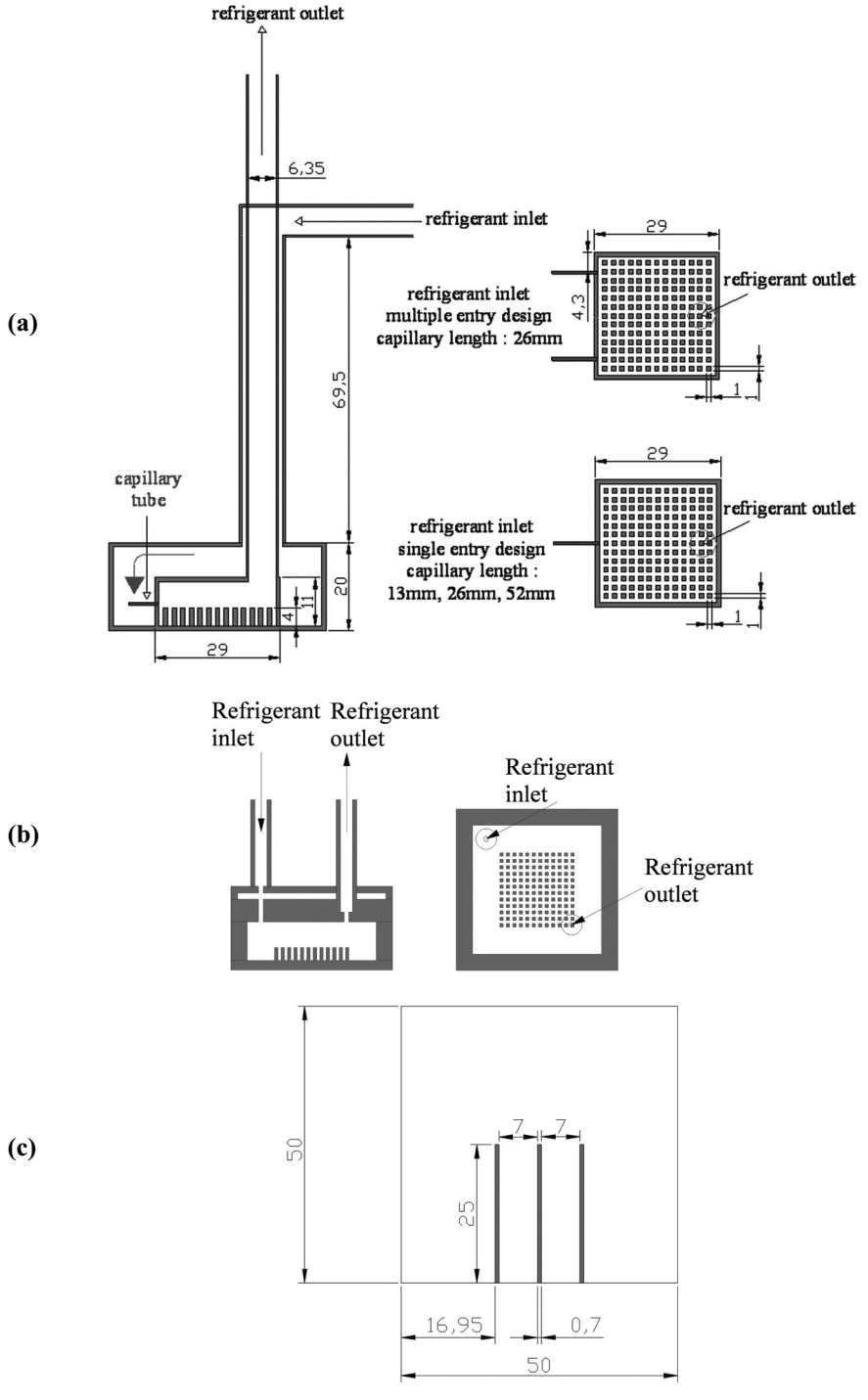

Figure 2. Schematic of the (a) proposed condensate-free cold plate, (b) conventional cold plate, and (c) detailed locations of the thermocouples placed beneath the base plate (units = mm).

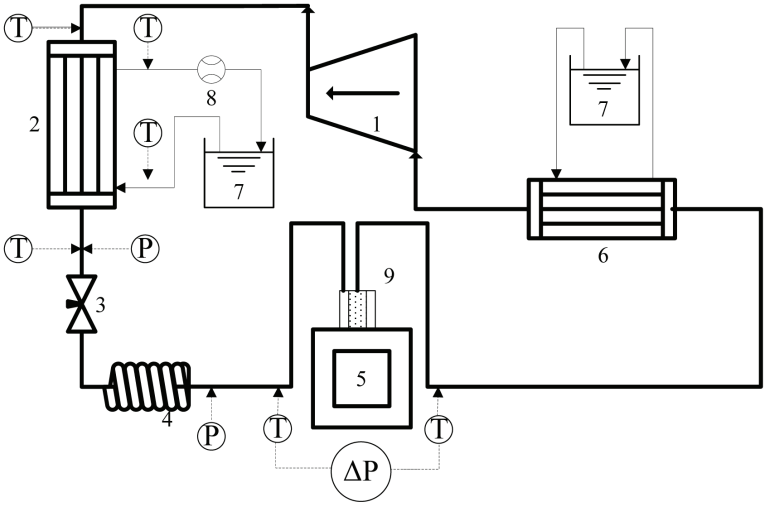

Legend: 1: compressor, 2: condenser, 3: metering valve, 4: capillary tube, 5: cold plate, 6: after-evaporator, 7: thermostat, 8. Cooling water flow meter, 9. Double pipe T: temperature sensor, P: pressure transducer, ΔP: differential pressure transducer.

Figure 3. Schematic of test setup.

300 mm (11.81 in.) is placed right after the metering valve. When the refrigerant leaves the capillary tube, it enters into the test cold plate. A total of five cold plates were made and tested for this study, including a conventional cold plate having only one container and four two-container designs to fulfill the proposed two-stage expansion concept. The two-stage expansion is made using either a single entry or multiple entries (two entries) at the second container. The lengths of the capillary tube for the single entry are 13 mm (0.51 in.), 26 mm (1.02 in.), and 52 mm (2.04 in.), and the capillary length of the dual entry is 26 mm (1.02 in.). The ID of the capillary tube is 0.5 mm (0.0197 in.). The cold plates contain an effective internal volume of 51 × 51 × 20 mm (2.01 × 2.01 × 0.79 in.). Detailed dimensions of the cold-plates are shown in Figures 2a–2b. A Kapton heater with an almost identical size (50.8 × 50.8 mm [3.16 × 3.16 in.]) to the cold plate is adhered below the cold plate to simulate the heat source. For measurement of the base temperature of the cold plates, three thermocouples are installed beneath the base plate. Detailed locations of the thermocouples are shown in Figure 2c. An insulation box made of Bakelite with a low thermal conductivity of 0.233 W/m·K (0.135 Btu/h·ft·°F) is placed beneath the heater to reduce heat loss. The heater is regulated with a DC power supply.

For recording the performance of the refrigeration system, two precise pressure transducers (YOKOKAWA, EJA530A with an accuracy of ±0.2%) are used to measure the condensing and evaporation pressure of the refrigerant system. A magnetic flowmeter (YOKOKAWA, ADMAGAE110MG) with a calibrated accuracy of 0.1% is employed to measure the water mass flow rate in the cooling loop of the condenser. Resistance temperature devices with a calibrated accuracy of 0.1°C (0.18°F) are installed at the refrigerant circuitry. The differential pressure transducers are YOKOKAWA EJA110A, which are accurate to 0.1% of the measuring span.

During the experiment, suitable adjustments of the system are made to ensure the inlet and outlet states of the condenser are in superheated and subcooled conditions. In the meantime, the heat capacity of the condenser can be obtained via the energy balance of the cooling water:

$$\dot{Q}_{cond} = \dot{m}_{water} c_p (T_{water,\,out} - T_{water,\,in}) \tag{1}$$

Apart from this condenser capacity, one can easily identify the enthalpy change of the refrigerant across the condenser through the measurement of the inlet and outlet states of condenser. Therefore, an estimation of the total refrigerant mass flow rate is made by the following relationship:

$$\dot{m}_{134a,\,total} = \frac{\dot{Q}_{cond}}{\Delta i_{cond}} \tag{2}$$

where Δi_{cond} represents the enthalpy difference of the refrigerant flow across condenser based on the measured inlet superheating and outlet subcooling temperatures. The overall uncertainty of the reduced mass flow rate is less than 4.8% throughout the test range.

The heat generated by the heater is then removed by cold plate, and the associated heat capacity of the cold plate with conventional expansion can be calculated as follows:

$$\dot{Q}_{evap} = \dot{m}_{134a,\,total}(i_3 - i_4) \tag{3}$$

The heat capacity of the cold plate with two-stage expansion can be calculated as follows:

$$\dot{Q}_{evap} = m_{134a,\,total}[(i_{3'} - i_{4'}) + (i_{4'} - i_{5'})] \tag{4}$$

Thus, the heat dissipating in the first container is denoted as $(i_{3'} - i_{4'})$ from internal heat transfer between refrigerant amid the first- and second-stage refrigerant. The heat loss can be obtained via the energy balance:

$$\dot{Q}_{loss} = \dot{Q}_{in} - \dot{Q}_{cond} \tag{5}$$

The heat loss is generally less than 10% and is regarded as a very minor loss. A T-S diagram of the influence of pressure drop subject to the second-stage expansion for the present two-container cold plate is shown in Figure 1. The refrigerant from the first-stage expansion is forced to pass through a short tube to perform the second-stage expansion. The calculation of the pressure drop in the two-phase flow system is very important in the design of the two-container cold plate. The frequently used methods to predict two-phase frictional pressure are separate flow model and homogeneous model (McAdams et al. 1949). Friedel (1979) proposed a separate model correlation containing a database of over 25,000 data points. The corresponding pressure drops can be calculated from the two-phase multiplier given by

$$\phi_{LO}^2 = \frac{dP_f / dz}{dP_{f,\,LO} / dz}\ , \tag{6}$$

where $dP_{f,LO}/dz$ is the frictional pressure gradient for the total flow assumed to be liquid. The homogeneous flow approximation treats the two-phase mixture as a single fluid with mixture properties, and it gives good predictions for smaller diameter tubes in both refrigerant and

air-water systems (Chen et al. 2002). In this study, we used both models to evaluate the pressure drops at the second-stage expansion.

RESULTS AND DISCUSSION

As previously mentioned, in the test facility a heater the same size as the cold plate is placed beneath the cold plate to simulate the heat source. During the experiments, the power is gradually increased to examine the response of the refrigeration system. For comparison purposes, we also performed tests for a conventional refrigeration system with a one-container cold plate; its schematic is shown in Figure 2b. Figure 4 shows the difference between this novel design and the conventional design during operation. Tests were conducted at the same environmental conditions. The ambient condition was maintained at T_{db} = 27°C±1°C (80.6°F±1.8°F) and RH = 55%±5%, where T_{db} is the dry-bulb temperature and RH denotes the relative humidity. As clearly seen in Figure 4a, humidification occurs at the outer surface of the conventional cold plate with condensate (or droplets) being easily identified. As seen in Figure 4b, no condensate forms outside the cold plate surface in the present two-stage design. In fact, with the double-pipe design, complete elimination of the condensate at the outlet connection piping is achieved.

For a more detailed comparison of the performance of the conventional cold plate with the present condensate-free cold plate design, one can see the associated variations (pressure/temperature) at the outlet vs. heat load in Figure 5. As seen in the outlet pressure in Figure 5a, there is a distinct difference between the two-stage cold plate and the conventional cold plate. For instance, the outlet pressure of the conventional cold plate holds rather steady when the supplied heat is lower than 100 W (0.095 Btu/s), yet it starts to rise for a further increase of supplied load. Notice that the length of the capillary tube is fixed (ID = 1.0 mm [0.0394 in.], length = 300 mm [11.81 in.]) for the conventional cold plate, thereby the refrigerant mass flow rate is roughly fixed for the conventional cold plate. In this regard, both the low-side pressure and the outlet temperature are increased provided the refrigerant is completely evaporated in the cold

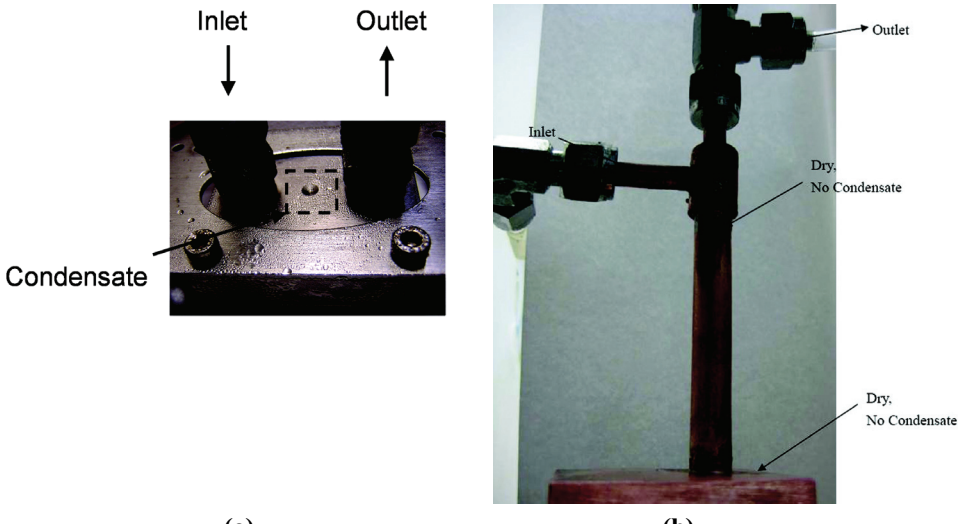

Figure 4. Typical test results of the present two-stage expansion concept relative to the conventional cold plate: (a) conventional design and (b) present design.

plate. This can be made clear from a considerable rise of outlet temperature when a heating load is raised above 150 W (0.142 Btu/s).

In the meantime, the two-stage expansion cold plate shows a quite distinct feature relative to that of the conventional design. As seen in Figure 5a, the low-side pressure is marginally increased or holds steady like a conventional cold plate with a small heating load, yet it starts to fall when the heating load increases. For the two-stage expansion design, adding flow resistance such as exploitation of a single capillary tube may accentuate the pressure decline. It is interesting that the outlet temperature of the two-stage cold plate holds quite steady (for multiple capillary

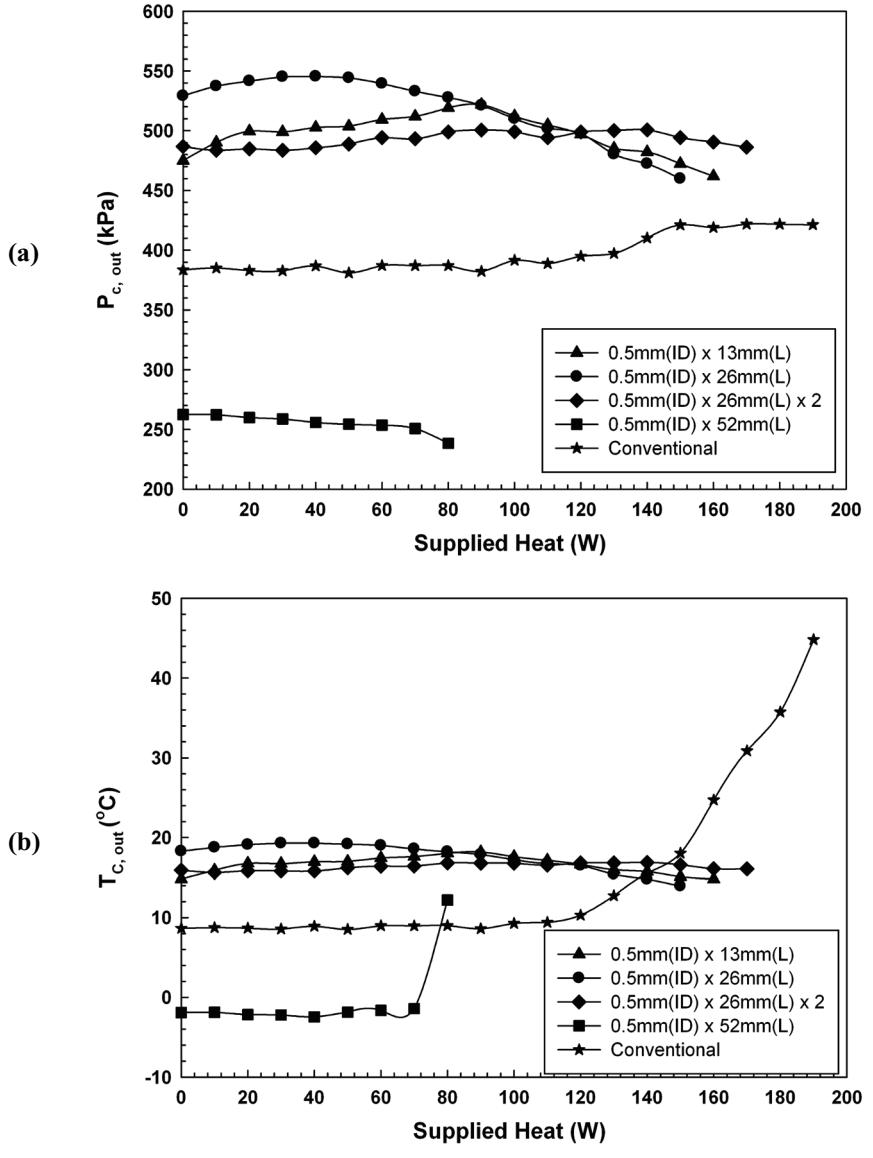

Figure 5. Detailed variations of the (a) outlet pressure and (b) outlet temperature subject to heating load between the conventional cold plate and the proposed novel design.

tubes or for a shorter capillary length) or even declines continuously with the rising load. This is because its continuously falling low pressure provides a larger temperature difference to redeem the increasing heat load, maintaining a lower and steady outlet temperature at the cold plate.

Figure 6 presents the wall temperature and pressure drop for the test cold plates. Considerably higher pressure drops for the present two-stage cold plate are seen relative to the conventional cold plate. Since refrigerant is being expanded when it flows into the first container, the two-phase flow entails more pressure loss as the refrigerant is required to contract itself into a

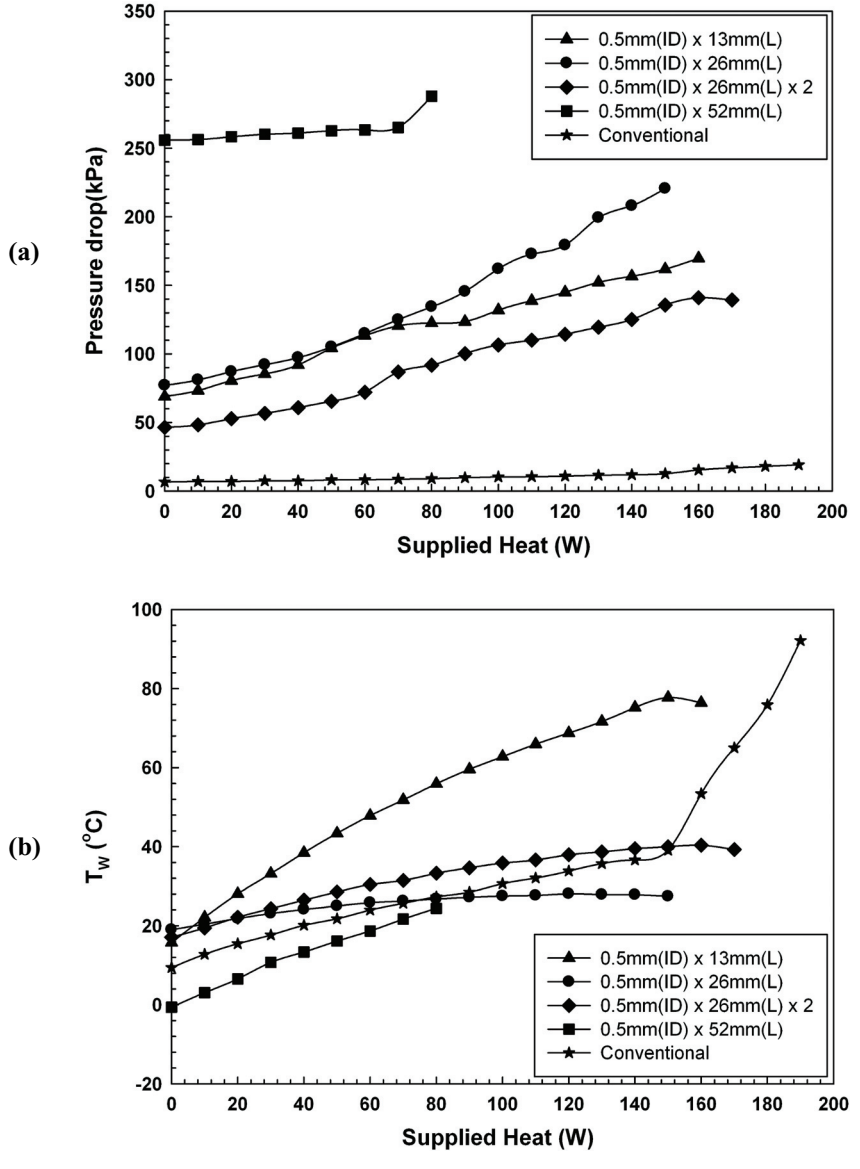

Figure 6. Detailed variations of the (a) pressure drop and (b) wall temperature subject to heating load between the conventional cold plate and the proposed novel design.

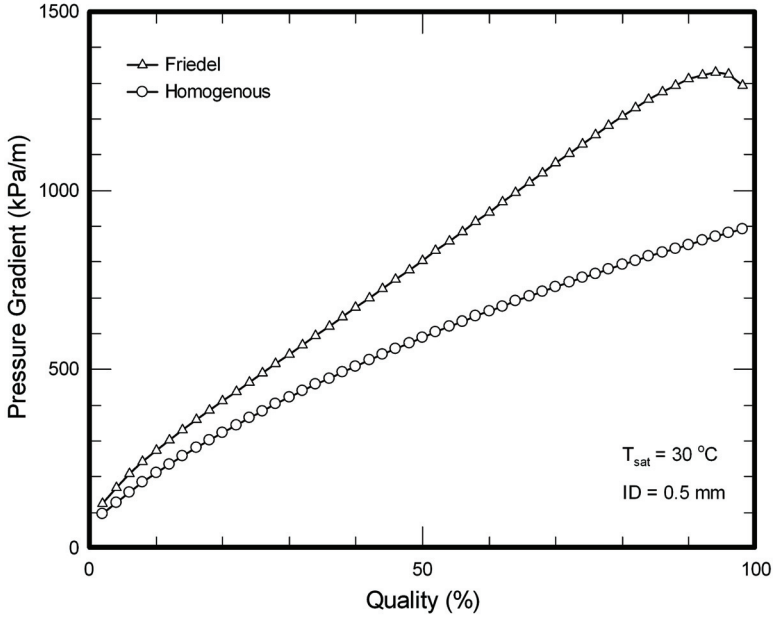

Figure 7. Influence of vapor quality on the pressure gradient for the R-134a refrigerant.

short capillary tube and to expand inside the second container. In this sense, a further rise in supplied heat engendered more refrigerant vapor within the first container, making the two-phase mixtures even harder to penetrate into the second container. As a consequence, one can see a continuous fall of low-side pressure and a considerable rise in pressure drop with increasing heat load for the two-stage design. The benefit of this design is that it could provide a comparatively fixed wall temperature/outlet refrigerant temperature of the cold plate, as shown in the figure. However, the down side for this design is that its significant increase in pressure drop in the first and second containers may lead to a blockage of two-phase mixture from the first container into the second container as it undergoes the second-stage expansion. Therefore, the endurable maximum supplied heat for the two-stage design is slightly lower than that of the convention design.

For further analysis of the effect of the two-stage design, the calculated results of pressure drop by the Friedel and homogenous models are shown in Figure 7. As shown, the pressure gradient ($\Delta P/\Delta z$) rises with vapor quality. With a longer capillary tube in the second-stage expansion, the appreciable pressure drop reduces the refrigerant mass flow rate accordingly. As a consequence, for a fixed heat load, refrigerant gives rise to a larger quality outlet and a much larger pressure drop between the two containers. In the meantime, there is a counterbalance from the effect between the pressure drop by quality and refrigerant mass flow rate. A rise in heating load leads to a larger superheated temperature, which is especially pronounced when the mass flow is low. Hence, one can see in Figure 6a that a longer capillary tube of 52 mm (2.05 in.) can reduce the outlet temperature to about –2°C (28.4°F). However, a much higher superheated state occurs when, due to its much lower mass flow rate, the system is unable to work when the maximum supplied heat is above 85 W (0.081 Btu/s). In summary, a longer capillary tube leads to a lower refrigeration temperature, a lower mass flow, and a smaller maximum heat capacity. To tackle this problem, one could employ a multiple short tube design.

CONCLUSION

Refrigeration is considered the potential solution for the needs of high flux cooling. However, there are several major concerns in the application of refrigeration systems to cool electronics. One of the major concerns is the condensate formation over the cold plate that may lead to potential failure of the electronics components/systems. In this study, we have proposed a two-stage expansion cold plate that is capable of reducing or even entirely eliminating the formation of condensate on the cold plate and connection piping. The design features a double-pipe inlet/outlet and a two-container cold plate design. The basic principle of this novel design makes use of a two-stage expansion. A capillary tube (or expansion valve) with a shorter length is placed after the condenser, thereby giving rise to a moderate pressure drop of the refrigerant from the condenser. The temperature is designated to be above the corresponding dew-point temperature of the ambient environment after first-stage expansion to eliminate the condensate problem. Inside the first container of the cold plate, the refrigerant then passes through a short tube to perform the second-stage expansion; the temperature of the refrigerant is then lowering further in the second container to perform heat exchange with the heat source. For complete removal of condensate formation from the whole refrigeration system, the present design uses a double-pipe inlet/outlet for the cold plate with the warmer refrigerant flowing into the cold plate being placed at the outer tube while the colder refrigerant vapor leaving the cold plate is placed in the inner tube. Through this design, the entire refrigeration system, including piping, is free from condensation formation.

A detailed comparison is also made between the conventional cold plate and the present condensate-free cold plate. For the conventional cold plate, the outlet pressure/temperature hold quite steady when the heat load is light, yet the outlet pressure/temperature show a substantial rise when the refrigerant is completely evaporated. In the meantime, the outlet pressure/temperature of the two-stage cold plate shows an opposite trend at a heavy heat load. The benefit of this characteristic is that the wall surface temperature and outlet temperature can be maintained comparatively steady.

ACKNOWLEDGMENTS

The authors are indebted to the financial support from the Bureau of Energy, the Ministry of Economic Affairs, Taiwan, and the 10% innovative funding from Industrial Technology Research Institute.

NOMENCLATURE

COP	=	coefficient of performance, dimensionless
c_p	=	specific heat, J/kg/K (Btu/lb$_m$/°F)
Δi_{cond}	=	enthalpy change across condenser, J/kg (Btu/lb$_m$)
dP/dz	=	two-phase pressure gradient, Pa/m (psi/ft)
$\dot{m}_{water}$	=	cooling water mass flow rate, kg/s (lb$_m$/s)
$\dot{m}_{134a,\,total}$	=	total refrigerant mass flow rate, kg/s (lb$_m$/s)
P	=	pressure, Pa (psi)
ΔP	=	pressure drop, Pa (psi)
$\dot{Q}_{cond}$	=	heat transfer rate at condenser, W (Btu/s)
$\dot{Q}_{evap}$	=	heat transfer rate at evaporator, W (Btu/s)
$\dot{Q}_{in}$	=	supplied heat, W (Btu/s)
$\dot{Q}_{loss}$	=	heat loss, W (Btu/s)
RH	=	relative humidity, %
S	=	entropy, J/K (Btu/°F)
T	=	temperature, °C (°F)
$T_{c,out}$	=	outlet temperature of cold plate, °C (°F)
T_w	=	wall temperature of cold plate, °C (°F)
T_{db}	=	dry-bulb temperature, °C (°F)
$T_{water,in}$	=	inlet temperature of cooling water, °C (°F)
$T_{water,outy}$	=	outlet temperature of cooling water, °C (°F)
ϕ_{LO}^2	=	two-phase friction multiplier for total flow assumed liquid, dimensionless

REFERENCES

Agwu Nnanna, A.G. 2006. Application of refrigeration system in electronics cooling. *Applied Thermal Engineering* 26:18–27.

Balestra, F., and G. Ghibaudo. 1994. Brief review of the MOS device physics for low temperature electronics. *Solid-State Electronics* 37:1967–1975.

Bash, C.E., C.D. Patel, and A. Beitelmal. 2002. Acoustic compression for the thermal management of multi-load electronic systems. *Proceedings of the Thermal and Thermomechanical Phenomena in Electronic Systems*, pp. 395–402.

Chen, I.Y., K.S. Yang, and C.C. Wang. 2002. An empirical correlation for two-phase frictional performance in small diameter tubes. *International Journal of Heat and Mass Transfer* 45:3667–71.

Friedel, L. 1979. Improved friction pressure drop correlations for horizontal and vertical two-phase pipe flow. European Two-Phase Group Meeting, Ispra, Italy, Paper E2.

Ghibaudo, G., F. Balestra, and A. Emrani. 1992. A survey of MOS device from low temperature electronics. *Microelectronic Engineering* 19:833–40.

McAdams, W.H., W.K. Woods, and L.C. Heroman, Jr. 1949. Vaporization inside horizontal tubes—II Benzene-oil mixtures, *Transactions of the ASME* 39:39–48.

Nnann, A.G.A. 2006. Application of refrigeration system in electronics cooling. *Applied Thermal Engineering* 26:18–27.

Phelan, P.E. 2001. Current and future miniature refrigeration cooling technologies for high power microelectronics. *Proceedings of Semiconductor Thermal Measurement & Management Symposium,* pp. 158–67.

Phelan, P.E., and J. Swanson. 2004. Designing a mesoscale vapor-compression refrigerator for cooling high-power microelectronic. *Proceedings of Intersociety Conference on Thermal and Thermomechanical Phenomena in Electronic Systems (I-THERM)*, pp. 218–23.

Schmidt, R.R., and B.D. Notohardjono. 2002. High-end server low-temperature cooling. *IBM Journal of Research and Development* 46:739–51.

Thermaltake. 2009. Thermaltake Xpressar. www.xpressar.com/index.html.

Taut, Y., D.A. Buchanan, W. Chen, D.J. Frank, K.E. Ismail, S. Lo, G.A. Sai-Halasz, R.G. Viswanathan, H.C. Warm, S.J. Wind, and H.Wong. 1997. CMOS scaling into the nanometer regime. *Proceedings of the IEEE 85*, No. 4, 486–504.

Asetek. The New VapoChill. www.tomshardware.com/reviews/processors-rocks,261-8.html.

Trutassanawin, S., E.A. Groll, S.V. Garimella, and L. Cremaschi. 2006. Experimental investigation of a miniature-scale refrigeration system for electronics cooling. *IEEE Transactions on Components and Packaging Technologies* 29:678–87.